

Magnetostriction and spin reorientation in ferromagnetic Laves phase $Pr(Ga_xFe_{1-x})_{1.9}$ compounds

Min-Yu Zeng(曾敏玉), Qing-Tang(唐庆), Zhi-Wei Mei(梅志巍), Cai-Yan Lu(陆彩燕), Yan-Mei Tang(唐妍梅), Xiang Li(李翔), Yun He(何云), and Ze-Ping Guo(郭泽平)

Citation: Chin. Phys. B, 2021, 30 (**6**): 067504. DOI: 10.1088/1674-1056/abe1a3
Journal homepage: http://cpb.iphy.ac.cn; http://iopscience.iop.org/cpb

What follows is a list of articles you may be interested in

Influence of Tb on easy magnetization direction and magnetostriction of $PrFe_{1.9}$ alloy

Chang-Xuan He(何昌璇), Yan-Mei Tang(唐妍梅), Xiang Li(李翔), Yun He(何云), Cai-Yan Lu(陆彩燕), Ze-Ping Guo(郭泽平)

Chin. Phys. B, 2019, 28 (**11**): 117501. DOI: 10.1088/1674-1056/ab47f6

Multiferroic and enhanced microwave absorption induced by complex oxide interfaces

Cuimei Cao(曹翠梅), Chunhui Dong(董春晖), Jinli Yao(幺金丽), Changjun Jiang(蒋长军)

Chin. Phys. B, 2018, 27 (**1**): 017503. DOI: 10.1088/1674-1056/27/1/017503

Low temperature magnetic and magnetostrictive properties in $Pr(Fe_{1-x}Co_x)_{1.9}$ cubic Laves alloys

Yan-Mei Tang(唐妍梅), Hang-Yu Xu(徐行翎), Ye Huang(黄业), Zhi-Xiong Tang(唐志雄), Shao-Long Tang(唐少龙)

Chin. Phys. B, 2017, 26 (**12**): 127502. DOI: 10.1088/1674-1056/26/12/127502

Modeling of the loading path dependent magnetomechanical behavior of Galfenol alloy

Hui Jiang(江慧), Jie Zhu(朱洁)

Chin. Phys. B, 2017, 26 (**3**): 037503. DOI: 10.1088/1674-1056/26/3/037503

Dy substitution effect on the temperature dependences of magnetostriction in $Pr_{1-x}Dy_xFe_{1.9}$ alloys

Yan-Mei Tang(唐妍梅), Hai-Fu Huang(黄海富), Shao-Long Tang(唐少龙), You-Wei Du(都有为)

Chin. Phys. B, 2016, 25 (**11**): 117503. DOI: 10.1088/1674-1056/25/11/117503

Magnetostriction and spin reorientation in ferromagnetic Laves phase $Pr(Ga_xFe_{1-x})_{1.9}$ compounds*

Min-Yu Zeng(曾敏玉)[1], Qing Tang(唐庆)[1], Zhi-Wei Mei(梅志巍)[1], Cai-Yan Lu(陆彩燕)[1], Yan-Mei Tang(唐妍梅)[1,†], Xiang Li(李翔)[2,‡], Yun He(何云)[1], and Ze-Ping Guo(郭泽平)[1]

[1] *Guangxi Key Laboratory of Nuclear Physics and Nuclear Technology, Guangxi Normal University, Guilin* 541004, *China*
[2] *School of Electronic Engineering and Automation, Guilin University of Electronic Technology, Guilin* 541004, *China*

(Received 16 November 2020; revised manuscript received 24 January 2021; accepted manuscript online 1 February 2021)

The magnetostriction, magnetization, and spin reorientation properties in $Pr(Ga_xFe_{1-x})_{1.9}$ alloys have been investigated by high-precision x-ray diffraction (XRD) step scanning, magnetization, and Mössbauer spectra measurements. Ga substitution reduces the magnetostriction ($\lambda_{||}$) with magnetic field $H \geq 8$ kOe (1 Oe = 1.33322×10^2 Pa), but it also increases the $\lambda_{||}$ value when $H \leq 8$ kOe at 5 K. Spin-reorientations (SR) are observed in all the alloys investigated, as determined by the step scanned XRD, Mössbauer spectra, and the abnormal temperature dependence of magnetization. An increase of the spin reorientation temperature (T_{SR}) due to Ga substitution is found in the phase diagram, which is different from the decrease one in many $R(T_xFe_{1-x})_{1.9}$ (T = Co, Al, Mn) alloys. The present work provides a method to control the easy magnetization direction (EMD) or T_{SR} for developing an anisotropic compensation system.

Keywords: easy magnetization direction (EMD), magnetostriction, spin-reorientation

PACS: 75.50.Bb, 75.80.+q **DOI:** 10.1088/1674-1056/abe1a3

1. Introduction

The binary C15 cubic Laves phase compound terfenol-D ($Tb_{0.27}Dy_{0.73}Fe_2$) is well known for its outstanding magnetostriction at room temperature, which is widely applied in acoustic transducers, sensors, and actuators.[1–3] However, the heavy rare earths are expensive, and their excellent magnetostrictive properties can only retain at the temperature range of −20 °C to +60 °C.[4,5] Therefore, the low-cost compound $PrFe_2$, which has large magnetostriction at a wide temperature range ($\lambda_{111} \sim 5600$ ppm at 0 K and $|\lambda_{||} - \lambda_{\perp}| \sim 1100$ ppm at room temperature) should be of giant interest.[1,6–8] However, the alloy also exhibits large magnetocrystalline anisotropy at low temperatures. Therefore, in the past decades, much efforts have been paid on developing a $R_xPr_{1-x}Fe_2$ anisotropic compensation system by selecting another RFe_2 alloy with different signs of magnetocrystalline anisotropy constant K_1 to $PrFe_2$ to obtain large magnetostriction at low magnetic fields.[9–17]

To develop a $R_xPr_{1-x}Fe_2$ anisotropic compensation system, the studies of crystal structures and spin reorientation temperature (T_{SR}) in $PrFe_2$ are significant. This is because for RFe_2 alloys, there is a one-to-one relationship between lattice distortion and EMD (rhombohedral structure with EMD along ⟨111⟩, orthorhombic structure with EMD along ⟨110⟩, and tetragonal structure with EMD along ⟨100⟩, respectively).[1,6,16–21] Besides, different EMDs correspond to different magnetocrystalline anisotropy properties, if K_2 and higher-order anisotropy constants are neglected.[21] $PrFe_2$ is a tetragonal symmetry below its T_{SR} (70 K) and a rhombohedral structure above its T_{SR}.[1,6–8,22] Then, another RFe_2 alloy considered in a $R_xPr_{1-x}Fe_2$ anisotropic compensation system should be selected basing on the crystal structure and T_{SR} of $PrFe_2$. For example, $TbFe_2$ with EMD lying along ⟨111⟩ should be considered when $T < 70$ K,[1,23,24] and $DyFe_2$ with EMD lying along ⟨100⟩ should be considered when 70 K$< T <$ 300 K, *etc*.[1,19]

As mentioned above, T_{SR} is an important property for $PrFe_2$ alloy, which significantly impacts the EMD and magnetic anisotropy. Low magnetocrystalline anisotropy frequently occurs at T_{SR}.[9–16] Therefore, it is of great interest if we find a method to control it for different temperature applications. According to the investigations of Ga substitution for Fe in $TbFe_2$ system, the EMD of the compound may deviate slightly from the major axis of symmetry, and it leads to the increase of tetragonal distortion λ_{100}.[25] Besides, the investigation of Ga substitution for Fe in $Dy_{0.6}Tb_{0.3}Pr_{0.1}(Fe_{0.95-x}Mn_{0.05}Ga_x)_{1.85}$ alloys shows that the substitution can affect the homogeneity region and the grain size of the multicomponent pseudobinary compound (Dy,Tb,Pr)(Fe,Mn,Ga)$_2$.[26] These results indicate that Ga substitution for Fe can impact the EMD or T_{SR} in the alloys. Then,

*Project supported by the National Natural Science Foundation of China (Grant No. 51901052), the Science Foundation of Guangxi Zhuang Autonomous Region, China (Grant No. 2018GXNSFAA281294), and the Training Programme for Thousands of Core Teachers in Guangxi Zhuang Autonomous Region, China.
†Corresponding author. E-mail: tangym0707@163.com
‡Corresponding author. E-mail: xli1984@hotmail.com
© 2021 Chinese Physical Society and IOP Publishing Ltd

we would like to examine here the effect of Ga substitution for Fe in the magnetic and magnetostriction properties, especially the EMD and T_{SR} in $PrFe_{1.9}$ alloy. Here, we choose the ratio of R:(Fe,Ga) as 1:1.9 instead of 1:2 in order to obtain a more pure Laves phase.[7,9]

2. Experiment design

We prepared the ingots of $Pr(Ga_xFe_{1-x})_{1.9}$ with $x = 0.0$, 0.02, 0.05, 0.10, and 0.15 stoichiometry by melting the high purity metals in a magneto controlled arc furnace in an argon atmosphere. The purities of the constituents are 99.9 wt%. Because the radius of Pr^{3+} is large, and the radius ratio of (R,Pr):Fe ion is too big to fit the ideal atomic radius ratio for Laves phase (1.225), the ingot were pressed to 6 GPa by a hexahedral anvil press and heated to 900 °C for 30 min to obtain single-phase Laves phase.[7,27] Conventional x-ray diffraction (XRD) analysis was carried out at room temperature using Cu $K\alpha$ radiation with a Rigaku D/Max-gA diffractometer. Figures 1(a) and 1(b) show the examples of XRD spectrum of $Pr(Ga_xFe_{1-x})_{1.9}$ compounds prepared under ordinary pressure and high pressure, respectively. The indices (hkl) of the Laves phase are also indexed here.[7,15,27,28] It can be seen from Fig. 1(a) that cubic Laves phase could hardly be observed in the samples prepared under ordinary pressure. However, all of the samples prepared by high-pressure annealing method exhibit almost single Cubic Laves phase with $MgCu_2$ structure, with minor impurity phases (*i.e.* rare-earth phases) over the whole concentration range investigated.[7,15,27,28] This indicates high-pressure annealing method is an effective method to prepare cubic Laves phase alloys with high content of Pr. The lattice parameters were calculated from the {220}, {311}, {422}, {333}, and {440} XRD spectra of Fig. 1(b) by Unit-Cell. The Curie temperature T_C was detected by a thermal gravitation analyzer (TGA) with a vertical gradient magnetic field under the samples. The Curie temperature T_C was determined by the differential thermal analysis (DTA). The crystal structure was determined by the Rigaku-TTR3 x-ray diffractometer. The scaling scale is from 40.5° to 43° for the {440} peak and from 70.5° to 73° for {222} peak, respectively, both with a step width of 0.02 between 15 K and 300 K. The x-ray diffraction (XRD) was performed with a fitted time mode, where each point was relaxed for 4 seconds. The XRD peaks were fitted by Jade 6.5 XRD analytical software, and the effect of the $K\alpha_2$ radiation was eliminated by a standard process. We used superconducting quantum interference device magnetometer (SQUID) to measure the temperature dependence of the magnetization (M) to determine T_{SR}. The magnetostrictions were measured using standard strain-gauge technique, while the magnetic fields were supplied by Quantum Design physical property measurement system (PPMS). The ^{57}Fe Mössbauer spectra were collected on a constant accelerated spectrometer with the transmission geometry at room temperature and 77 K, with the source of ^{57}Co in Pd matrix with an activity of about 25 mCi. The spectrums were calibrated with a standard α-Fe foil and analyzed by Lorentzian lines in 256 channels using the software Klencsar and Moss-Winn.

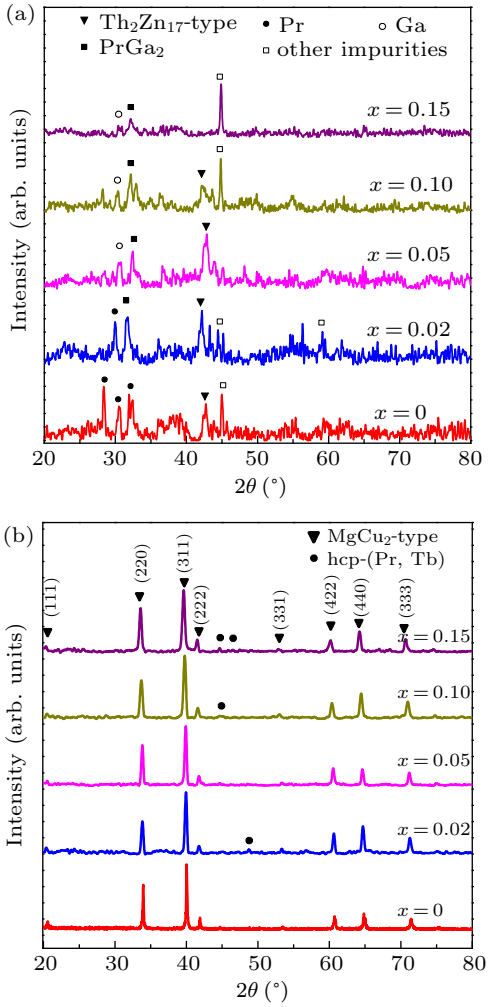


Fig. 1. XRD patterns of $Pr(Ga_xFe_{1-x})_{1.9}$ compounds prepared (a) under ordinary pressure and (b) high pressure, respectively.

3. Results and discussion

In order to detect the Curie temperature T_C of $Pr(Fe_{1-x}Ga_x)$ alloys, the thermo gravimetric analysis (TGA) was performed, and the results are shown in Fig. 2. Then T_C was determined by the differential thermal analysis (DTA), which is shown in the inset of Fig. 2 (taking the alloy with $x = 0.02$ as an example).

The concentration dependence of T_C is plotted in Fig. 3. It can be found in Fig. 3 that T_C decreases from 513 K to 433 K with increasing Ga concentration x, which can be probably attributed to the decrease of R–T coupling strength due to Ga substitution. It is similar to the results of $Tb(Fe_{1-x}Ga_x)$[25] and $Dy_{0.6}Tb_{0.3}Pr_{0.1}(Fe_{0.95-x}Mn_{0.05}Ga_x)_{1.85}$ alloys.[26] The lattice parameter a calculated from the XRD spectra (Fig. 1(b)) is

also plotted in Fig. 3. The lattice parameter increases from 0.746 nm to 0.753 nm with increasing Ga content, which can be attributed to the larger atom radius of Ga compared to that of Fe. This result is also similar to that of $Tb(Fe_{1-x}Ga_x)$[25] and $Dy_{0.6}Tb_{0.3}Pr_{0.1}(Fe_{0.95-x}Mn_{0.05}Ga_x)_{1.85}$ alloys.[26]

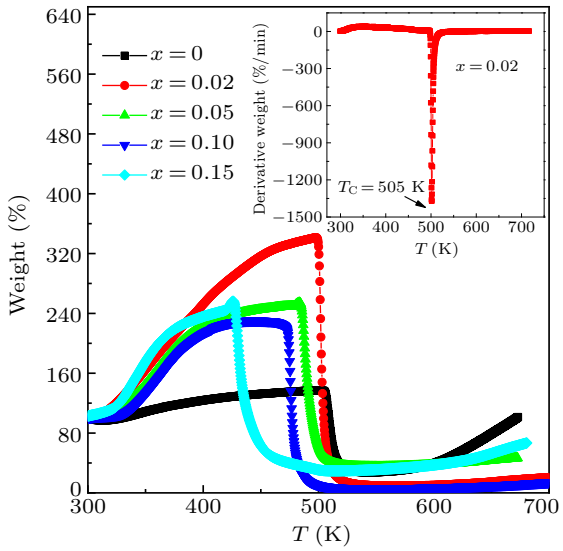


Fig. 2. The TGA of $Pr(Ga_xFe_{1-x})_{1.9}$ alloys. The inset shows the differential thermal analysis of the alloy with $x = 0.02$.

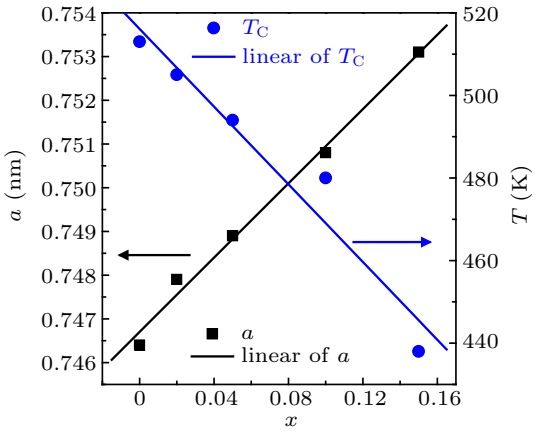


Fig. 3. Ga concentration dependence of lattice parameter a and Curie temperature T_C, respectively.

Figure 4 shows the magnetic field dependence of magnetostriction $\lambda = (\lambda_{||} - \lambda_{\perp})$ at both room temperature and 5 K, respectively. As shown in Fig. 4(a), the magnetostriction decreases monotonously with the increasing x at room temperature (RT), due to the decrease of magnetic properties of the compounds.[1,25,26] Once again, this result is similar to that of $Tb(Fe_{1-x}Ga_x)$[25] and $Dy_{0.6}Tb_{0.3}Pr_{0.1}(Fe_{0.95-x}Mn_{0.05}Ga_x)_{1.85}$ systems.[26] However, at 5 K, Ga substitution reduces the magnetostriction when 10 kOe $\leq H \leq$ 90 kOe, while it yields an increased magnetostriction with 0 kOe $\leq H \leq$ 10 kOe, as shown in the inset of Fig. 4(b). This indicates that Ga substitution with $0.02 \leq x \leq 0.05$ can enhance the magnetostriction at 5 K.

Figure 5 shows the magnetization (M) temperature dependence of the alloys at the magnetic field of 50 kOe. An abnormity can be seen clearly in the magnetization (M) curve for each compounds, which has been marked by an arrow in the figure. By comparing the M–T data with those obtained from the high-precision XRD step scanning,

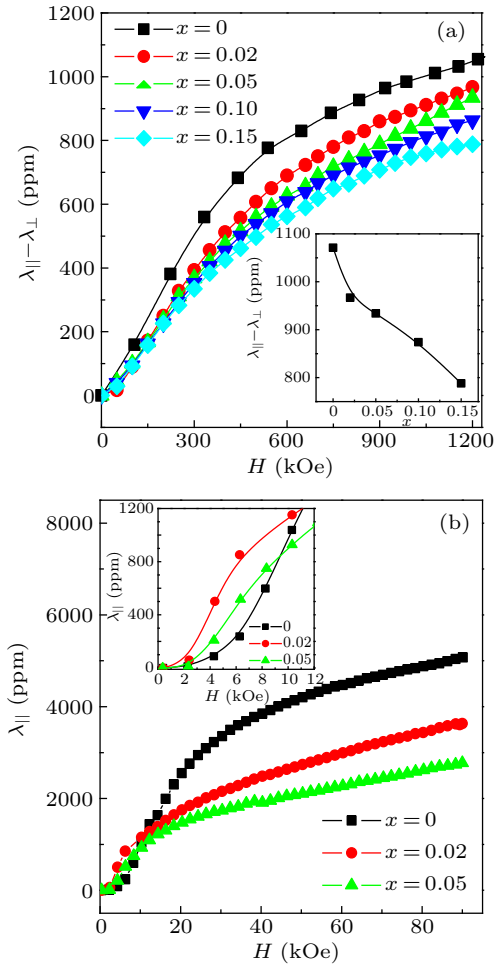


Fig. 4. (a) The field dependence of magnetostriction ($\lambda = \lambda_{||} - \lambda_{\perp}$) at RT. (b) The field dependence of the magnetostriction ($\lambda_{||}$) at 5 K of $Pr(Ga_xFe_{1-x})_{1.9}$ alloys. The inset shows $\lambda_{||}$ with 0 kOe $\leq H \leq$ 12 kOe.

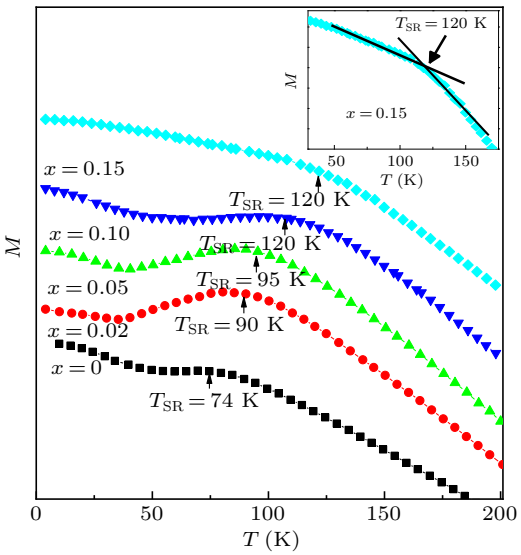


Fig. 5. Temperature dependence of the magnetization (M) for the alloys with $x = 0.0$, 0.02, 0.05, 0.10, and 0.15, respectively, at the field strength $H = 50$ kOe. The inset shows the determination of T_{SR} when $x = 0.15$.

as well as our earlier reported Mössbauer spectra measurements, we are able to identify the anomalies corresponding to the spin reorientations.[8,10,13,16–20,29,30] For $x = 0$, an anomaly appears in the form of a peak at 74 K, which is identified as a spin reorientation taking place from ⟨100⟩ to ⟨111⟩. Then this anomalies seems to shift to approximately 120 K when x increases from 0.0 to 0.15. The anomaly for $x = 0.15$ is not very obvious, but it can be observed in an enlarged view as shown in the inset of Fig. 5, which is similar to the situations of $Sm_{0.76}Nd_{0.24}Fe_2$ and $Sm_{0.7}Nd_{0.3}Fe_2$.[29]

In order to further confirm the EMD type in Ga-containning alloys above and below the anomalies temperature in M–T curve, a high-precision XRD step scanning was performed on $Pr(Ga_{0.02}Fe_{0.98})_{1.9}$ for the {222} and {440} peaks during cooling from 300 K to 15 K after elimination of $K\alpha_2$, which are shown in Figs. 6(a) and 6(b), respectively. The double-splitting of the {222} and {440} reflections (the intensity ratio of split peaks is about 1:3 and 1:1, respectively) between 135 K and 300 K are typical for rhombohedral structure,[1,6–8,19,20] indicating the EMD of the compound lies along ⟨111⟩ in this temperature range. On the other hand, a prominent tetragonal symmetry can be seen between 15 K and 80 K, which can be confirmed by the non-splitting of the {222} reflections and doubly splitting of the {440} reflections. This indicates the EMD of the compound lies along ⟨100⟩ in this temperature range. Thus we can conclude that the spin-reorientation occurs in the $Pr(Ga_{0.02}Fe_{0.98})_{1.9}$ alloy, which has been verified in Pr-containning alloys.[1,6–8]

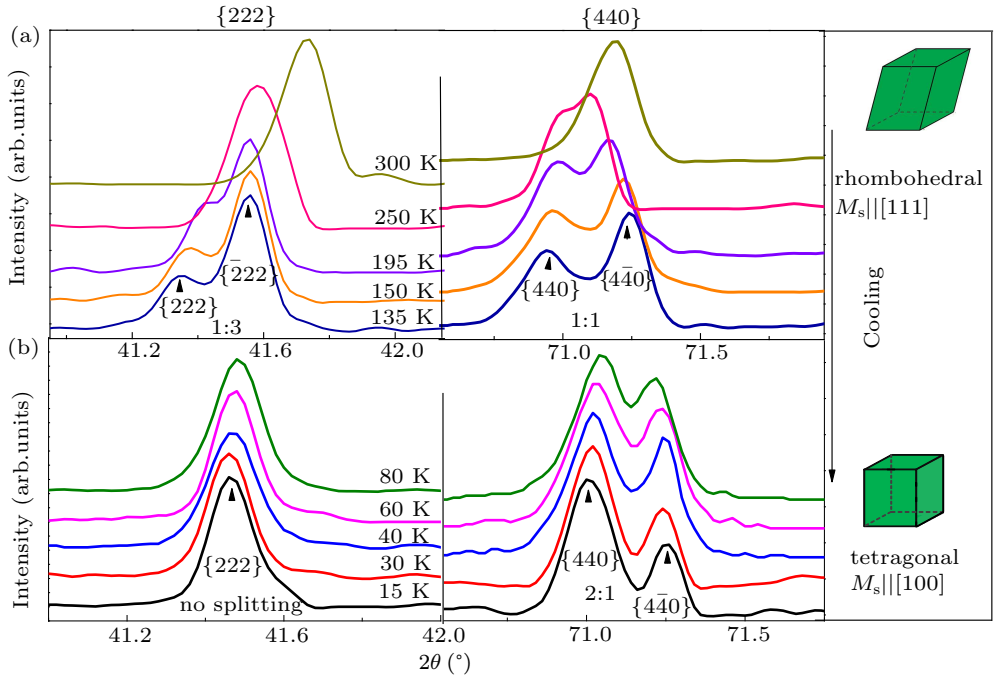


Fig. 6. The profiles of the step-scanned {440} and {222} XRD reflection of the sample with $x = 0.02$.

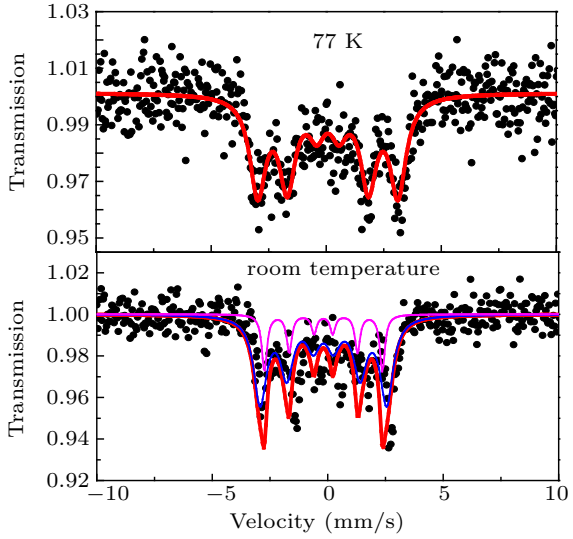


Fig. 7. ^{57}Fe Mössbauer spectra of $Pr(Ga_{0.02}Fe_{0.98})_{1.9}$ at 77 K and room temperature, respectively.

Figure 7 shows the ^{57}Fe Mössbauer spectra for single-phase $Pr(Ga_{0.02}Fe_{0.98})_{1.9}$ at both 77 K and room temperature, where the circles present the experimental data and the solid lines give the fitted curves. The data can be fitted by two sextets with area ratio about 3:1 at room temperature, indicating that the EMD is along the ⟨111⟩ axis.[9,22,23,31] On the other hand, for the data at 77 K, the spectra can be fitted by a single sextet, indicating that EMD is lying along ⟨100⟩. These results are in good agreement with the XRD result in Fig. 6. Therefore, the abnormities in magnetization (M) results in Fig. 5 can be explained by the transform of EMD from ⟨111⟩ to ⟨100⟩ in the alloys.

The phase diagram of the spin configuration accompanied with different structures for $Pr(Ga_xFe_{1-x})_{1.9}$ alloys are plotted in Fig. 8, in which T_{SR} is obtained from the collection of the M–T curve in Fig. 5 and T_C is obtained from the

collection of the DTA data in Fig. 3. Meanwhile, the EMD type were determined by XRD (Fig. 6) and Mössbauer spectra measurements (Fig. 7), and were represented by red circle, blue trigon, light blue diamond, and pink trigon, respectively. It can be seen from Fig. 8 that the phase diagram can be separated into three regions, which have been identified by cubic symmetry region I, rhombohedral symmetry region II, and tetragonal symmetry region III, respectively. It can be seen that the EMD types accurately land in the corresponding region ($\langle 111\rangle$ in region II and $\langle 100\rangle$ in region III). This indicates that the data from XRD and Mössbauer spectra measurement are well consistent with the T_{SR} determined by M–T curve. Furthermore, it shows that T_C decreases with increasing Ga concentration x, due to the decrease of R–T coupling strength caused by Ga substitution.[19,20] An increase of T_{SR} from 70 K to 120 K can be seen in Fig. 8, with the increasing Ga concentration x. It indicates that the 3d–4f hybridization or even 4f–4f coupling is composition-sensitive in this system.[25,26] This result is similar to that of Co or Al substitution for Fe in light rare earth Laves phase compounds, such as $Pr_{0.5}Nd_{0.5}(Fe_{1-x}Co_x)_{1.9}$,[16] $Nd(Fe_{1-x}Co_x)_{1.9}$,[32] $Pr(Fe_{1-x}Co_x)_{1.9}$,[33] and $Pr(Fe_{1-x}Al_x)_{1.9}$ systems.[34] However, it is different to that in $Tb_{0.3}Dy_{0.7}(Fe_{1-x}Mn_x)_2$,[35] and $Sm_{0.88}Dy_{0.12}(Fe_{1-x}Co_x)_2$ systems,[36] in which Co or Mn substitution for Fe slightly decreases T_{SR}. The underlying physical mechanisms is still to be investigated.

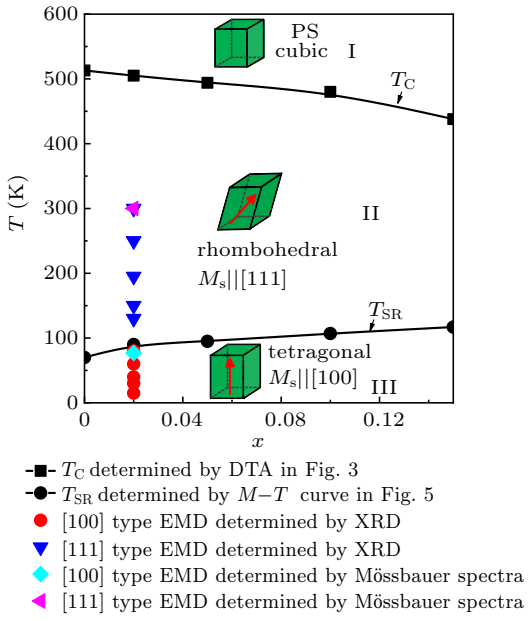


Fig. 8. Phase diagram of the spin configuration accompanied with different crystal structures for $Pr(Ga_xFe_{1-x})_{1.9}$ compounds (M_s denotes the easy magnetization direction, PS denotes the paramagnetic state).

The intrinsic magnetostriction λ_{111} of the $PrFe_{1.9}$ and $Pr(Ga_{0.02}Fe_{0.98})_{1.9}$ as a function of temperature is shown in Fig. 9, in which λ_{111} was obtained from

$$\lambda_{111} = 2\frac{d_{440} - d_{4\bar{4}0}}{d_{440} + d_{4\bar{4}0}}$$

with d_{440} and $d_{4\bar{4}0}$ denoting the crystallographic plane distances of $\{440\}$ and $\{4\bar{4}0\}$, respectively. The parameters d_{440} and $d_{4\bar{4}0}$ can be calculated by the Bragg's formula $\lambda = 2d\sin\theta$ (λ represents the wavelength, θ represents the angle of diffraction in Fig. 7).[6,9,30] The data of λ_{111} in $PrFe_{1.9}$ were obtained from Ref. [8]. The error of λ_{111} was estimated by the error transfer formula

$$\Delta\lambda_{111} = \sqrt{\left(\frac{\partial\lambda_{111}}{\partial\theta_1}\right)^2\Delta\theta_1^2 + \left(\frac{\partial\lambda_{111}}{\partial\theta_2}\right)^2\Delta\theta_2^2},$$

in which θ_1 and θ_2 stand for the diffraction angles of $\{440\}$ and peaks, respectively, and the scanning angle error is $\Delta\theta = 0.02^\circ/2$. Significant decrease of λ_{111} with increasing temperature can be observed in both samples, which can be attributed to the rapid decrease of the sublattice moment with decreasing temperature.[1] Ga substitution yields a rapid decrease spontaneous magnetostriction λ_{111}. This is similar to the result of Ga substitution for Fe in $TbFe_2$. which can be explained by the single-ion model.[25,26] According to the single-ion model, λ_{111} varies with temperature as magnetic moment $\sigma_R^3(T)$. Assuming the rare earth sublattice moment decreases with decreasing Curie temperature T_C, the decrease of T_C with increasing Ga content results in a decrease of $\sigma^3(T)$, which leads to a reduction in the spontaneous magnetostriction λ_{111}.

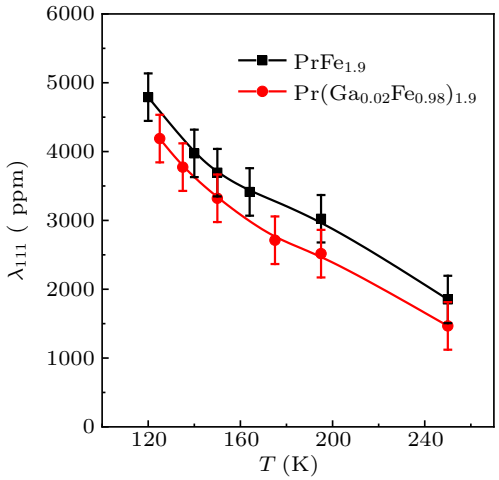


Fig. 9. Temperature dependence of the spontaneous magnetostriction λ_{111} for $PrFe_{1.9}$ and $Pr(Ga_{0.02}Fe_{0.98})_{1.9}$.

4. Conclusions

Ga substitution decreases the magnetostriction with magnetic field of $H \geq 8$ kOe, while increases the magnetostriction when 0 kOe$\leq H \leq 8$ kOe for the compounds with $x \leq 0.05$ at 5 K. Drastic transition of the step scanned XRD and Mössbauer spectra, as well as the abnormal temperature dependence of magnetization and magnetostriction are observed, which indicate the occurrence of spin-reorientation (SR) in all the alloys investigated. The phase diagram is constructed, which illustrates an increase of the spin-reorientation temperature T_{SR} due to Ga substitution.

References

[1] Clark A E 1980 *Ferromagnetic Materials*, Vol. 1, ed. Wohlfarth E P (Amsterdam: North-Holland) p. 531
[2] Koon N, Williams C and Das B 1991 *J. Magn. Magn. Mater.* **100** 173
[3] Callen E 1969 *Proceedings of the Metallic Magnetoacoustic Materials Workshop*, edited by F S Garter (Boston: Office of Naval Research, Arlington, VA)
[4] Clark A E, Teter J P and Wun-Fogle 1991 *J. Appl. Phys.* **69** 5771
[5] Clark A E, Teter J P and McMasters O D 1988 *J. Appl. Phys.* **63** 3910
[6] Ren W J and Zhang Z D 2013 *Chin. Phys. B* **22** 077507
[7] Shi Y G, Tang S L, Huang Y J, Nie B, Qian B, Lv L Y and Du Y W 2007 *J. Alloys Compd.* **443** 11
[8] Tang Y M, Chen L Y, Zhang L, Huang H F, Xia W B, Zhang S Y, Wei J, Tang S L and Du Y W 2014 *J. Appl. Phys.* **115** 173902
[9] Ren W J, Zhang Z D, Zhao X G, Liu W and Geng D Y 2004 *Appl. Phys. Lett.* **84** 562
[10] Ren W J, Li D, Liu W, Li J and Zhang Z D 2008 *J. Appl. Phys.* **103** 07B311
[11] Li F, Liu J J, Zhu X Y, Shen W C, Lin L L, Du J and Si P Z 2018 *Solid State Commun.* **275** 63
[12] Lin L L, Liu J J, Shen W C, Ding Q L, Wang M K, Du J and Si P Z 2018 *Appl. Phys. A* **124** 706
[13] Ren W J, Liu J J, Li D, Liu W, Zhao X G and Zhang Z D 2006 *Appl. Phys. Lett.* **89** 122506
[14] Shi Y G, Tang S L, Zhai L, Huang H B, Wang R L, Yu J Y and Du Y W 2008 *Appl. Phys. Lett.* **92** 212507
[15] Ren W J, Li D, Sui Y C, Liu W, Zhao X G, Liu J J, Li J and Zhang Z D 2006 *J. Appl. Phys.* **99** 08M701
[16] Hu C C, Shi Y G, Chen Z Y, Shi D N, Tang S L and Du Y W 2014 *J. Alloys Compd.* **613** 153
[17] Wang Y, Tang S L, Li Y L, Xie R and Du Y W 2013 *Chin. Phys. B* **22** 037503
[18] Yang S, Bao H X, Zhou C, Wang Y, Ren X B, Yoshitaka Matsushita, Yoshio Katsuya, Masahiko Tanaka, Keisuke Kobayashi, Song X P and Gao J R 2010 *Phys. Rev. Lett.* **104** 197201
[19] Shi Y G, Chen Z Y, Wang L, Hu C C, Pan Q and Shi D N 2016 *AIP Adv.* **6** 056207
[20] Wang Y, Ma T Y, Wu C, Yan M, Zhang C S, Chen X P, Sun G G, Yang S, Wang Y, Chang T Y, Zhou C, Liao X Q and Zheng X Q 2017 *AIP Adv.* **7** 075311
[21] Ren W J, Yang J L, Li B, Li D, Zhao X G and Zhang Z D 2009 *Physica B* **404** 3410
[22] M Shimotomai, H Miyake and M Doyama 1980 *J. Phys. F: Met. Phys.* **10** 707
[23] Shi Y G, Tang S L, Huang Y J, Lv L Y and Du Y W 2007 *Appl. Phys. Lett.* **90** 142515
[24] Murtaza Adil, Yang S, Zhou C and Song X P 2016 *Chin. Phys. B* **25** 096107
[25] Tang Y J, Feng Y B, Luo H L and Pan S M 1994 *J. Appl. Phys.* **76** 7145
[26] Tang S L, Wu C H, Jin X M, Wang B W, Chuang Y C, Li J Y and Zhao X G 1996 *J. Alloys Compd.* **242** 114
[27] Zhao X G, Li J Y, Liu S C, Ji S Q and Jia K C 1997 *J. Alloys Compd.* **258** 39
[28] Pan Z B, Liu J J, Si P Z and Ren W J 2016 *Mater. Res. Bull.* **77** 122
[29] Wang Y, Ren W J, Yang Y H, Li B, Li J and Zhang Z D 2013 *J. Appl. Phys.* **113** 143903
[30] Liu X Y, Liu J J, Pan Z B, Song H X, Zhang Z R, Du J and Ren W J 2015 *J. Magn. Magn. Mater.* **391** 60
[31] Li F, Liu J J, Zhang Z R, Lin L L, Shen W C, Zhu X Y, Du J and Si P Z 2017 *J. Alloys Compd.* **725** 946
[32] Hu C C, Shi Y G, Zheng T F, Fan J Y, Shi D N, Lv L Y and Tang S L 2012 *J. Appl. Phys.* **112** 063902
[33] Tang Y M, Xu H Y, Huang Y, Tang Z X and Tang S L 2017 *Chin. Phys. B* **26** 127502
[34] Tang Y M, Chen L Y, Wei J, Tang S L and Du Y W 2014 *Chin. Phys. B* **23** 077503
[35] Funayama T, Kobayashi T, Sakai I and Sahashi M 1992 *Appl. Phys. Lett.* **61** 114
[36] Guo H Q, Gong H Y, Yang H Y, Li Y F, Yang L Y, Shen B G and Li R Q 1996 *Phys. Rev. B* **54** 4107